Programmable pH-Triggered DNA Nanoswitches

Andrea Idili,[†,‡] Alexis Vallée-Bélisle,*,[§] and Francesco Ricci*,[†,‡]

[†]Dipartimento di Scienze e Tecnologie Chimiche, University of Rome, Tor Vergata, 00133, Rome, Italy

[‡]Consorzio Interuniversitario Biostrutture e Biosistemi "INBB", Rome, Italy

[§]Laboratory of Biosensors and Nanomachines, Département de Chimie, Université de Montréal, Québec, Canada

Ⓢ *Supporting Information*

ABSTRACT: We have designed programmable DNA-based nanoswitches whose closing/opening can be triggered over specific different pH windows. These nanoswitches form an intramolecular triplex DNA structure through pH-sensitive parallel Hoogsteen interactions. We demonstrate that by simply changing the relative content of TAT/CGC triplets in the switches, we can rationally tune their pH dependence over more than 5 pH units. The ability to design DNA-based switches with tunable pH dependence provides the opportunity to engineer pH nanosensors with unprecedented wide sensitivity to pH changes. For example, by mixing in the same solution three switches with different pH sensitivity, we developed a pH nanosensor that can precisely monitor pH variations over 5.5 units of pH. With their fast response time (<200 ms) and high reversibility, these pH-triggered nanoswitches appear particularly suitable for applications ranging from the real-time monitoring of pH changes in vivo to the development of pH sensitive smart nanomaterials.

Nature often employs finely pH-regulated biomolecules to modulate and tune a number of biological activities[1] ranging from enzyme catalysis[2] to protein folding,[3] membrane function,[4] and apoptosis.[5] For these reasons, developing probes, switches, or nanomaterials that are able to respond to specific pH changes should prove useful for several applications in the fields of in vivo imaging, clinical diagnostics, and drug delivery.[6-8]

By taking advantage of the high versatility and designability of DNA chemistry[9-19] several groups have recently developed pH-triggered DNA-based probes or nanodevices.[20-30] Such probes typically exploit DNA secondary structures that display pH dependence due to the presence of specific protonation sites. These structures include I-motif,[21-23,26,29,31] intermolecular triplex DNA,[25,28,32] DNA tweezers,[20] and, more recently, the A-motif.[33] Despite the promising and advantageous characteristics of some of these DNA-based nanodevices, which include fast response times and sustained efficiency over several cycles, a drawback inevitably affects their performances: they all respond (with an exception[33a]) over a fixed pH window that typically spans 1.5−2 pH units.[26,34,33b] These nanodevices, thus, cannot be adapted to provide a useful output outside these fixed pH windows.

Here we describe a method to rationally design and program pH-triggered DNA-based nanoswitches whose pH dependence

can be finely tuned and edited over more than 5 units of pH. We created our switches by taking advantage of the well-characterized pH sensitivity of the parallel Hoogsteen (T,C)-motif in triplex DNA.[34-36] To do so, we designed a DNA-based triplex pH-triggered nanoswitch that consists in a double intramolecular hairpin stabilized with both Watson−Crick (W−C) and parallel Hoogsteen interactions (Figure 1). More
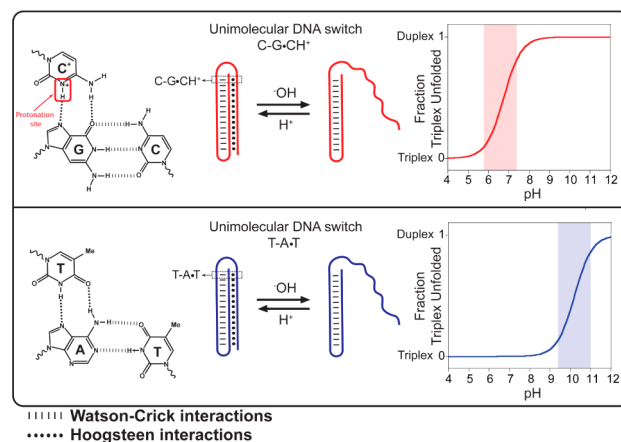

Figure 1. Programmable DNA-based triplex pH-triggered nanoswitches that form an intramolecular triplex structure through the formation of a W−C (dashed) pH-insensitive hairpin and a second Hoogsteen (dots) pH-sensitive hairpin. Because they require the protonation of the N3 of cytosine in the third strand (top, left), CGC triplets are only stable at acid pHs (average pK_a of protonated cytosines in triplex structure is ≈6.5).[35] For this reason, triplex switches containing only CGC triplets should unfold into an open duplex conformation at slightly acidic pHs. Bottom: In contrast, triplex switches containing only TAT triplets should unfold at much higher pHs due to deprotonation of thymine (pK_a ∼ 10).[39c]

specifically, one hairpin of the triplex nanoswitch is formed by the W−C hybridization of two 10 base complementary portions separated by a 5 base loop. This duplex DNA is then able to form a triplex structure via the formation of a second hairpin through Hoogsteen parallel interactions with the other extremity of the switch (Figure 1).[37] Importantly for our work, while W−C base pairings are almost insensitive to pH,[34] Hoogsteen interactions show a strong and variable pH dependence.[34-36] More specifically, the CGC parallel triplet requires the protonation

of the N3 of cytosine in the third strand in order to form (average pK_a of protonated cytosines in triplex structure is ≈ 6.5[35,38]) (Figure 1, top). In contrast, the TAT triplets are relatively stable at neutral pH and are only destabilized at pH above 10 due to the deprotonation of thymine ($pK_a \sim 10$)[39c] (Figure 1, bottom). To follow opening/closing of the triplex portion of the switch, we labeled it with a fluorophore/quencher pair. More specifically, a fluorophore is conjugated at one end of the DNA sequence, and a quencher is internally inserted in the loop of the hairpin duplex DNA so that the triplex-to-duplex transition (unfolding) brings the fluorophore away from the quencher and increases the fluorescence signal observed (Figure 2). We note that the fluorophore used in this work (Alexa Fluor 680) is insensitive to pH over a wide pH window (Figure S1).[40]
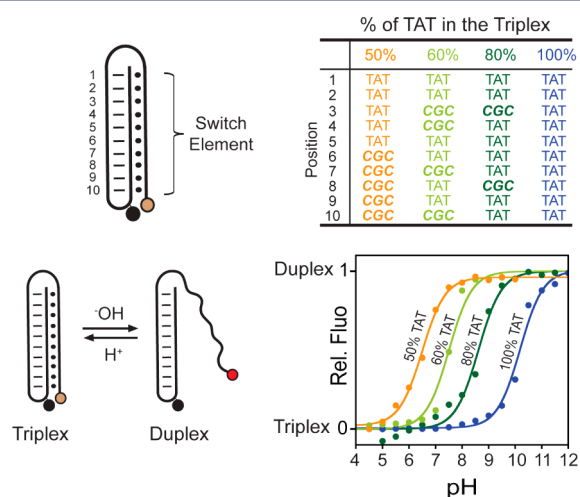

Figure 2. Top: Triplex pH nanoswitches can be rationally programmed to be triggered over a specifically defined pH window. The pH sensitivity of the triplex interactions can be tuned by changing the CGC vs TAT content of the switch element, thus allowing to tune the pH window at which the triplex-to-duplex transition occurs (bottom, right). The opening of the switch containing only TAT triplets (100% TAT, blue curve), for example, is triggered at basic pHs (9−11), while the triplex structure of a switch with a 50% content of TAT (50% TAT, orange curve) unfolds at a more acidic pH range (5−7). Switches with TAT contents between 50% and 100% show intermediate pH sensitivity. Shown are the pH−titration curves (bottom, right) of the triplex nanoswitches (at 20 nM concentration) achieved in an universal citrate/phosphate/borate buffer[41] at 25 °C. Triplex-to-duplex transition is monitored through a pH-insensitive fluorophore (Alexa Fluor 680) inserted at the 5′-end and a quencher (Black-Hole Quencher 2, BHQ-2) internally located in the switch. We note that the W−C-stabilized hairpin remains folded over the wide range of pH investigated (Figure S3).

Our DNA-based triplex nanoswitch is sensitive to pH. We first tested a switch containing an equal distribution of TAT and CGC triplets (50% TAT) (Figure 2, orange curve). As expected, at very acidic pH values, the intramolecular double hairpin triplex structure is favored, and we observe a very low fluorescence signal (fluorophore and quencher are brought in close proximity). As we increase the pH of the solution, the triplex structure is destabilized, and we observe a gradual increase of the fluorescence signal characteristic of the triplex-to-duplex transition (unfolding). pH of semiprotonation (defined here as pK_a^{obs}, the average pK_a due to several interacting protonation sites) for this triplex nanoswitch is 6.5.

We can tune the pH dependence of our switches over a window of more than 5 units of pH by simply changing the relative content of CGC/TAT triplets in the sequence. For example, when the switch element contains only TAT triplets (100% TAT i.e., without any CGC triplet), the triplex-to-duplex transition occurs at basic pHs ($pK_a^{obs} = 10.2$) (Figure 2, blue curve). By gradually replacing TAT triplets with CGC triplets, we can precisely program the switch so that it opens at a specific lower pH. By replacing 2 TAT triplets with 2 CGC triplets in the switch element's sequence, e.g., we reduce the pK_a^{obs} of the switch from 10.2 to 8.6 (80% TAT, Figure 2, dark-green curve). The addition of four CGC triplets in the sequence further moves the pK_a^{obs} down to 7.5 (60% TAT, Figure 2, light green curve). Finally, as shown above, a switch with an equal content of CGC vs TAT triplets shows a complete opening at slightly acidic pHs ($pK_a^{obs} = 6.5$) (50% TAT, Figure 2, orange curve). Triplex nanoswitches with higher CGC percentage content in the sequence (i.e., 20% and 0% TAT) show the same pH dependence of the one containing an equal content of CGC vs TAT (50% TAT) (Figure S4). The modulated pH dependence at different TAT/CGC contents might be explained by several factors. In the presence of low CGC content (i.e., 80% TAT) the pK_a observed (8.6) is higher than that of the free cytosine ($pK_a \sim 4.5$) probably because of the predominant effect of the pH-insensitive TAT triplets ($pK_a \sim 10.2$). On the other hand, as soon as 50% of the switch is composed of CGC triplets (i.e., 50, 20, 0% TAT), its pK_a reaches a minimal value of ~ 6.5 (Figure S4). This pK_a value remains, however, relatively higher than that of the free protonated cytosine likely due to both the stabilization provided by the formation of the Hoogsteen interactions (hydrogen bonds) and to the increase of base triplet stacking interactions in the switch.[38]

The possibility to design triplex nanoswiches with tunable pH dependence provides the opportunity to engineer pH sensors with unprecedented wide sensitivity to pH changes. As it is the case for most DNA-based pH-triggered nanodevices,[26,33b,34] our programmable triplex nanoswitches show a limited and fixed dynamic range (defined here as the pH range at which the switches display 10−90% of their maximum signal) which spans ~ 1.8 units of pH (see, e.g., 50% TAT, Figure 3, left). This, in turn, corresponds to a change of $[H^+]$ concentration of 81-fold which represents the classic dynamic range window (the range of
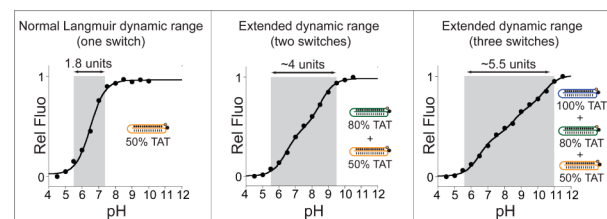

Figure 3. By combining together two or more switches, we can create a pH-sensor displaying extended dynamic ranges. Left: A single switch shows a typical fixed dynamic range of ~ 1.8 units of pH (here the 50% TAT is only an example, see also Figure 2). Center: By combining in the same solution two switches (i.e., 50% TAT and 80% TAT), each triggered over pH windows that are 2 orders of magnitude apart[43] (see Figure 2), we can extend the useful dynamic range to ~ 4 units of pH. Right: It is possible to further extend the useful pH dynamic range (~ 5.5 units of pH) by using together in the same solution three different switches (50%, 80%, and 100% TAT). Shown are the pH−titration curves obtained using a universal citrate/phosphate/borate buffer and a total concentration of triplex nanoswitches of 20 nM (see SI for details).

ligand concentration over which receptor occupancy shifts from 10% to 90%) inherent to single-site binding and Langmuir binding curves.[42] This fixed window can hinder the applicability of our switches where changes over a wider range of pH require to be monitored with precision. To overcome this problem, we propose to extend this dynamic range by combining together two or more switches triggered over different pH windows.[43] For example, by combining together the 50% TAT and 80% TAT switches we created a pH sensor with a dynamic range that spans ~4.0 units of pH (from 5.5 to 9.5) (Figure 3, center). A dynamic range of similar width, but shifted to more basic pHs (from 7.5 to 11.0), is also observed when combining the 80% TAT and 100% TAT switches (Figure S5). Finally, by combining together three switches (50%, 80%, and 100% TAT), we created a pH sensor displaying a dynamic range of ~5.5 units of pH (from 5.5 to 11.0).

Our switches respond to pH changes in milliseconds. We demonstrate this by performing stopped-flow experiments and by measuring the opening/closing reaction rates of each switch over its relevant pH dynamic range (Figures S6–S12). All switches show opening/closing kinetics (average time constant ~100 ms) sufficiently fast to allow the real time monitoring of pH variation in the millisecond range. Switches with a content of 20%, 60%, and 80% TAT display measurable kinetics (see Figure S6 and Table S1). In contrast, switches with a content of 0%, 50%, and 100% TAT display kinetics so fast (<3 ms) that their folding/unfolding transitions could not be determined using a conventional stopped-flow instrument.

The switches are reversible and only respond over a specific pH window. To demonstrate this, we selected three switches that are triggered over three well-separated pH windows (20%, 60%, and 100% TAT, see Figures 2 and S2) and tested them with a series of cyclic pH-jump experiments (Figure 4). In the first experiment, for example, the pH of the three solutions containing the switches (each solution containing a different switch) was cycled from pH 5.0 to 7.0 and back to pH 5.0 for five times (see Figure 4, top). Only the 20% TAT switch was triggered over this pH window, while the other two switches (60% and 100% TAT) did not give any significant signal change. In the other two series of experiments (Figure 4, center and bottom), we selected different pH jumps to trigger only one switch. In all three experiments we observed a high reversibility of the switches' signal and a minimal cross-activation coming from the other two switches. A similar experiment was carried out with these same switches but this time by mixing them in equimolar amount in the same solution. The pH of the solution was cyclically changed to unfold/fold only one switch at a time (Figure S13). As expected, the fluorescence change observed was consistent with the opening/closing of a single switch thus further demonstrating both the reversibility and specificity of our triplex nanoswitches.

Here we designed programmable DNA-based triplex nanoswitches whose folding/unfolding can be triggered at specific pH values. The nanoswitches form an intramolecular triplex DNA structure and take advantage of the pH dependence of parallel Hoogsteen interactions. We demonstrated that we could tune the pH sensitivity of these switches by simply changing the relative content of TAT/CGC triplets in the sequence. For example, switches with a high CGC content (≥50%) are opened near a pH of ~5.5–6.0, while switches with lower CGC content (<50%) are opened at gradually more basic pHs. A switch that does not contain CGC triplets (and thus only contains TAT triplets, 100% TAT), for example, starts unfolding only at pH above 10.0. The ability to design nanoswitches with defined pH
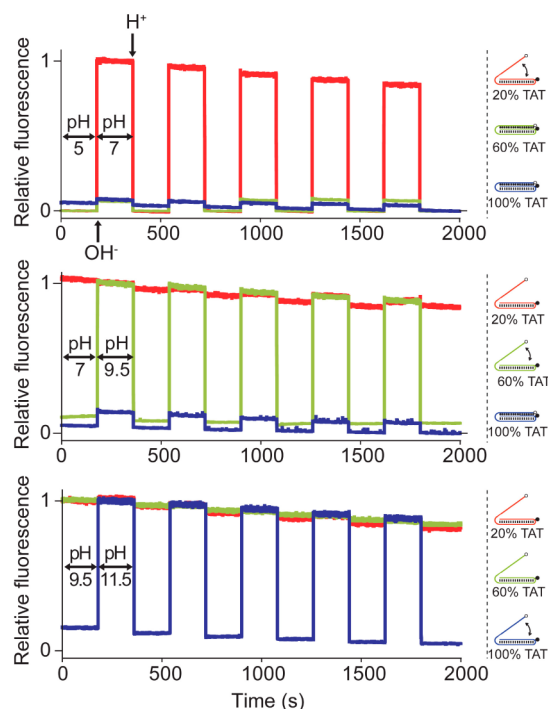

Figure 4. Triplex pH nanoswitches show high reversibility and no cross-activation. This is demonstrated by cyclically changing the pH of three solutions each containing a single switch (20%, 60%, and 100% TAT). Top: Cycling the pH from 5.0 to 7.0 (and vice versa) only activates the most unstable switch (20% TAT, red line), while no significant signal is observed for the switches with higher TAT content (60% TAT, 100% TAT). Center: A pH change from 7.0 to 9.5 leads to opening/closing of only the 60% TAT switch (green line). Within this pH window, the 100% TAT switch (blue line) remains closed, while the 20% TAT switch is already completely open. Bottom: When the pH solution is cycled between 9.5 and 11.5, we observe the opening/closing transition of the 100% TAT (blue line), while the other two switches are already completely open within this pH range. Each solution contains only one switch (20 nM), and the pH of the solution was cyclically changed by adding small aliquots of 3 M NaOH or HCl. In this experiment we selected the 20% TAT switch over the 50% TAT switch (Figures 2 and 3), because the former displays a slightly steeper dose–response curve (see Figure S2) which better prevents cross-activation. The small drift of fluorescence signal observed over time is due to photobleaching of the fluorophore (Alexa Fluor 680) under the experimental conditions we used (see Figure S14).

sensitivity offers several advantages. For example, a switch can be developed and optimized for a specific application that requires monitoring variations of pH over only a specific range. Similarly, we demonstrated that by mixing in the same solution two or more switches, each with a different pH sensitivity, we can obtain pH sensors with extended dynamic range. Using this strategy, we achieved an unprecedented wide pH window of 5.5 units over which these switches respond robustly. Moreover, with their nanosize, fast response time (<100 ms) and high reversibility, the triplex pH-triggered nanoswitches appear particularly suitable for applications including the real-time monitoring of pH changes in cellular extracts, in in vivo cells[8,18c,26] or in other media where pH changes represent an important input both in healthy and pathological biological pathways.[44] For example, because pH dysregulation is an hallmark of cancer, and many cancers are characterized by an inverted pH gradient between the inside and the outside of cells,[44] our switches could be of value for diagnostic purposes. Finally, the ability to program DNA strands

to open/close over a specific pH window could find many applications in the field of DNA nanomachines,[45] drug delivery systems,[46] and smart nanomaterials.[47]

ASSOCIATED CONTENT

Ⓢ Supporting Information

Methods and figures. This material is available free of charge via the Internet at http://pubs.acs.org.

AUTHOR INFORMATION

Corresponding Authors

francesco.ricci@uniroma2.it

a.vallee-belisle@umontreal.ca

Notes

The authors declare no competing financial interest.

ACKNOWLEDGMENTS

REFERENCES

(1) (a) Lukin, J. A. *Chem. Rev.* **2004**, *104*, 1219. (b) McLachlan, G. D.; Cahill, S. M.; Girvin, M. E.; Almo, S. C. *Biochemistry* **2007**, *46*, 6931.

(2) (a) Nishi, T.; Forgac, M. *Nat. Rev. Mol. Cell Biol.* **2002**, *3*, 94. (b) Slepkov, E. R.; Rainey, J. K.; Sykes, B. D.; Fliegel, L. *Biochem. J.* **2007**, *401*, 623.

(3) Matsuyama, S.; Llopis, J.; Deveraux, Q. L.; Tsien, R. Y.; Reed, J. C. *Nat. Cell Biol.* **2000**, *2*, 318.

(4) (a) Paroutis, P.; Touret, N.; Grinstein, S. *Physiology* **2004**, *19*, 207. (b) Busa, W. B.; Nuccitelli, R. *Am. J. Physiol.* **1984**, *246*, R409.

(5) Tews, I.; Findeisen, F.; Sinning, I.; Schultz, A.; Schultz, J. E.; Linder, J. U. *Science* **2005**, *308*, 1020.

(6) Zhou, K.; Liu, H.; Zhang, S.; Huang, X.; Wang, Y.; Huang, G.; Sumer, B. D.; Gao, J. *J. Am. Chem. Soc.* **2012**, *134*, 7803.

(7) Gallagher, F. A.; Kettunen, M. I.; Day, S. E.; Hu, D. E.; Ardenkjær-Larsen, J. H.; Zandt, R.; Jensen, P. R.; Karlsson, M.; Golman, K.; Lerche, M. H.; Brindle, K. M. *Nature* **2008**, *453*, 940.

(8) Modi, S.; Nizak, C.; Surana, S.; Halder, S.; Krishnan, Y. *Nat. Nanotechnol.* **2013**, *8*, 459.

(9) Bath, J.; Tuberfield, A. J. *Nat. Nanotechnol.* **2007**, *2*, 275.

(10) Seeman, N. C. *Annu. Rev. Biochem.* **2010**, *79*, 65.

(11) Dittmer, W. U.; Reuter, A.; Simmel, F. C. *Angew. Chem., Int. Ed.* **2004**, *43*, 3550.

(12) Wieland, M.; Benz, A.; Haar, J.; Halder, K.; Hartig, J. S. *Chem. Commun.* **2010**, *46*, 1866.

(13) Zhou, C.; Yang, Z.; Liu, D. *J. Am. Chem. Soc.* **2012**, *134*, 1416.

(14) Thomas, J. M.; Yu, H. Z.; Sen, D. *J. Am. Chem. Soc.* **2012**, *134*, 13738.

(15) Li, X. M.; Li, W.; Ge, A. Q.; Chen, H. Y. *J. Phys. Chem. C* **2010**, *114*, 21948.

(16) McLaughlin, C. K.; Hamblin, G. D.; Sleiman, H. F. *Chem. Soc. Rev.* **2011**, *40*, 5647.

(17) (a) Teller, C.; Willner, I. *Curr. Opin. Biotechnol.* **2010**, *21*, 376. (b) Andersen, E. S. *Nat. Biotechnol.* **2010**, *31*, 184. (c) Zhang, D. Y.; Winfree, E. *J. Am. Chem. Soc.* **2008**, *130*, 13921. (d) Greschner, A.; Bujold, K.; Sleiman, H. F. *J. Am. Chem. Soc.* **2013**, *135*, 11283.

(18) (a) Simmel, F. C. *Angew. Chem., Int. Ed.* **2008**, *47*, 5884. (b) Krishnan, Y.; Simmel, F. C. *Angew. Chem., Int. Ed.* **2011**, *50*, 3124.

(c) Bhatia, D.; Sharma, S.; Krishnan, Y. *Curr. Opin. Biotechnol.* **2011**, *22*, 475.

(19) Vallée-Bélisle, A.; Ricci, F.; Plaxco, K. W. *Proc. Natl. Acad. Sci. U.S.A.* **2009**, *106*, 13802.

(20) (a) Shimron, S.; Magen, N.; Elbaz, J.; Willner, I. *Chem. Commun.* **2011**, *47*, 8787. (b) Elbaz, J.; Want, Z. G.; Orbach, R.; Willner, I. *Nano Lett.* **2009**, *9*, 4510.

(21) Li, T.; Famulok, M. *J. Am. Chem. Soc.* **2013**, *135*, 1593.

(22) Liu, D.; Balasubramanian, S. *Angew. Chem., Int. Ed.* **2003**, *115*, 5912.

(23) Liu, D.; Bruckbauer, A.; Abell, C.; Balasubramanian, S.; Kang, D.; Klenerman, D.; Zhou, D. *J. Am. Chem. Soc.* **2006**, *128*, 2067.

(24) Zhou, J.; Amrane, S.; Korkut, D. N.; Bourdoncle, A.; He, H. Z.; Ma, D. L.; Mergny, J. L. *Angew. Chem., Int. Ed.* **2013**, *52*, 7742.

(25) Brucale, M.; Zuccheri, G.; Samorì, B. *Org. Biomol. Chem.* **2005**, *3*, 575.

(26) Modi, S.; Swetha, M. G.; Goswami, D.; Gupta, G. D.; Mayor, S.; Krishnan, Y. *Nat. Nanotechnol.* **2009**, *4*, 325.

(27) Chen, L.; Di, J.; Cao, C.; Zhao, Y.; Ma, Y.; Luo, J.; Wen, Y.; Song, W.; Songd, Y.; Jiang, L. *Chem. Commun.* **2011**, *47*, 2850.

(28) Chen, Y.; Lee, S-H.; Mao, C. *Angew. Chem., Int. Ed.* **2004**, *43*, 5335.

(29) Wang, W.; Yang, Y.; Cheng, E.; Zhao, M.; Meng, H.; Liu, D.; Zhou, D. *Chem. Commun.* **2009**, *7*, 824.

(30) Liedl, T.; Simmel, F. C. *Nano Lett.* **2005**, *5*, 1894.

(31) Liu, H.; Xu, Y.; Li, F.; Yang, Y.; Wang, W.; Song, Y.; Liu, D. *Angew. Chem., Int. Ed.* **2007**, *46*, 2515.

(32) (a) Han, X.; Zhou, Z.; Yang, F.; Deng, Z. *J. Am. Chem. Soc.* **2008**, *130*, 14414. (b) Kolaric, B.; Sliwa, M.; Brucale, M.; Vallée, R. A. L.; Zuccheri, G.; Samori, B.; Hofkensa, J.; De Schryver, F. C. *Photochem. Photobiol. Sci.* **2007**, *6*, 614. (c) Li, X. M.; Song, J.; Cheng, T.; Fu, P. Y. *Anal. Bioanal. Chem.* **2013**, *405*, 5993.

(33) (a) Saha, S.; Chakraborty, K.; Krishnan, Y. *Chem. Commun.* **2012**, *48*, 2513. (b) Chakraborty, K.; Sharma, S.; Maiti, P. K.; Krishnan, Y. *Nucleic Acids Res.* **2009**, *97*, 2810.

(34) Ohmichi, T.; Kawamoto, Y.; Wu, P.; Miyoshi, D.; Karimata, H.; Sugimoto, N. *Biochemistry* **2005**, *44*, 7125.

(35) Leitner, D.; Schroder, W.; Weisz, K. *Biochemistry* **2000**, *39*, 5886.

(36) Sugimoto, N.; Wu, P.; Hara, H.; Kawamoto, Y. *Biochemistry* **2001**, *40*, 9396.

(37) (a) Sklenar, V.; Feigon, J. *Nature* **1990**, *345*, 836. (b) Haner, R.; Dervan, P. B. *Biochemistry* **1990**, *29*, 9761. (c) Volker, J.; Botes, D. P.; Lindsey, G. G.; Klump, H. H. *J. Mol. Biol.* **1993**, *230*, 1278.

(38) (a) Asensio, J. S.; Lane, A. N.; Dhesi, J.; Bergqvist, S.; Brown, T. *J. Mol. Biol.* **1998**, *275*, 811. (b) Husler, P. L.; Klump, H. H. *Arch. Biochem. Biophys.* **1995**, *317*, 46. (c) Soto, A.; Loo, J.; Marky, L. *J. Am. Chem. Soc.* **2002**, *124*, 14355.

(39) (a) Liu, Z.; Li, Y.; Tian, C.; Mao, C. *Biomacromolecules* **2013**, *14*, 1711. (b) Keppler, M. D.; Fox, K. R. *Nucl. Acid Res.* **1997**, *25*, 4644. (c) Saenger, W. *Principles of Nucleic Acid Structure*; Ch. R. Cantor, Ed.; Springer: New York, 1984.

(40) Panchuk-Voloshina, N.; Haugland, R. P.; Bishop-Stewart, J.; Bhalgat, M. K.; Millard, P. J.; Mao, F.; Leung, W. Y.; Haugland, R. P. *J. Histochem. Cytochem.* **1999**, *47*, 1179.

(41) Östling, S.; Virtama, P. *Acta Phys. Scandinav.* **1946**, *11*, 289.

(42) (a) Ferrell, J. E., Jr. *Trends Biochem. Sci.* **1996**, *21*, 460. (b) Goldbeter, A.; Koshland, D. E., Jr. *Q. Rev. Biophys.* **1982**, *15*, 555.

(43) (a) Vallée-Bélisle, A.; Ricci, F.; Plaxco, K. W. *J. Am. Chem. Soc.* **2012**, *134*, 2876. (b) Porchetta, A.; Vallée-Bélisle, A.; Plaxco, K. W.; Ricci, F. *J. Am. Chem. Soc.* **2012**, *134*, 20601.

(44) Webb, B. A.; Chimenti, M.; Jacobson, M. P.; Barber, L. P. *Nat. Rev.* **2011**, *11*, 671.

(45) (a) Turberfield, J.; Mitchell, J. C.; Yurke, B.; Mills, A. P.; Blakey, M. I.; Simmel, F. C. *Phys. Rev. Lett.* **2003**, *90*, 118102−118105. (b) Simmel, F. C. *Nanomedicine* **2007**, *2*, 817.

(46) Bae, Y.; Fukushima, S.; Harada, A.; Kataoka, K. *Angew. Chem., Int. Ed.* **2003**, *42*, 4640.

(47) Du, J.; Du, X.; Mao, C.; Wang, J. *J. Am. Chem. Soc.* **2011**, *133*, 17560.